Proaromatic pyranylidene chalcogen analogues and cyclopenta[c]thiophen-4,6-dione as electron donors and acceptor in efficient charge-transfer chromophores

Parmeshwar Solanke [a, b], Sylvain Achelle [a, *], Nolwenn Cabon [a], Oldřich Pytela [b],
Alberto Barsella [c], Bertrand Caro [a], Françoise Robin-le Guen [a], Jan Podlesný [b],
Milan Klikar [b], Filip Bureš [b, **]

[a] Institut des Sciences Chimiques de Rennes UMR CNRS 6226, IUT de Lannion, rue Edouard Branly, BP 30219, F22302 Lannion Cedex, France
[b] Institute of Organic Chemistry and Technology, Faculty of Chemical Technology, University of Pardubice, Studentská 573, Pardubice 53210, Czech Republic
[c] Département d'Optique ultra-rapide et Nanophotonique, IPCMS-CNRS, 23 Rue du Loess, BP 43, 67034 Strasbourg Cedex 2, France

ABSTRACT

Fifteen new push-pull chromophores based on a proaromatic pyranylidene donor and its chalcogen analogues and various electron acceptor moieties were synthesized in a straightforward manner. These model molecules were designed and prepared to investigate the concept of proaromaticity as a tool to tune the fundamental properties of push-pull systems. All target chromophores with systematically varied structure were further investigated by electrochemistry, absorption spectra, and EFISH experi-ment in conjunction with DFT calculations. Employing structural variations such as chalcogen/acceptor replacement, extension of the π-system, and the position of substitution along the pyran ring, the HOMO-LUMO gap can be tuned within the range of 2.18 to 1.41 eV. A new and powerful electron withdrawing moiety, combining features of polarizable thiophene and successful indane-1,3-dione acceptor, cyclopenta[c]thiophen-4,6-dione (ThDione) has also been developed.

Keywords: Chalcogenopyranylidene Push-pull; Non linear optics Charge transfer Polymethines

1. Introduction

During the past decades, there has been a great interest for molecular systems displaying second-order nonlinear optical (NLO) responses due to their application in a wide range of electronic and optoelectronic devices. The most common design of organic chro-mophores exhibiting 2nd order NLO properties consists of push-pull systems with an electron-donor group (D) attached to an electron-accepting group (A) via a π-conjugated core (D-π-A design) [1]. Intramolecular charge transfer (ICT) in such D-π-A systems leads to polarization of the chromophore and generation of a molecular dipole. The ICT can easily be illustrated by two limiting resonance forms (aromatic and quinoid/zwitterionic arrangement) [2]. The D–A interaction generates new low-energy molecular orbital, which accounts for the unique and peculiar properties of

push–pull chromophores such as intensive color, electrochemical behavior, crystallinity, intermolecular interactions as well as NLO properties [3]. Microscopically, the 2nd order nonlinearity of chromophores can be represented by the scalar product of the vector part of the hyperporalizability tensor (β) and the dipole moment (μ) [4].

α- and γ-pyranylidene fragments are six membered chalcogen-containing heterocycles which possess an exocyclic double bond at either the C2 or the C4 positions, respectively. Due to the presence of an intracyclic heteroatom in conjugation with the unsaturated carbon backbone, pyranylidenes are considered as good electron-donors depending on the substituent(s) attached to the C=C exocyclic double bond. The pyranylidene fragment generally acts as proaromatic electron donor in push-pull molecules [5], which, upon the ICT, gain a pyrylium aromatic character. Hence, pyr-anylidene may impart very strong mesomeric effect depending on the strength of the acceptor group A attached and the length/nature of the unsaturated π-spacer used. The donor capacity of pyr-anylidene fragments is also exemplified by the chemical or elec-trochemical oxidation of the methylenepyran moiety leading to a

radical cation which dimerizes to bispyrylium and extended bis-pyrans [6]. Incorporation of pyranylidene fragment within the structure of NLOphores [7] and organic chromophores for dye sensitized solar cells (DSSCs) [8] has already been described in the literature. However, replacement of chalcogen atoms within the γ-pyranylidene fragment has been much less studied [9]. In addition, α-pyranylidene fragments have never been used in a push-pull structure for NLO.

Activated methylene derivatives such as malononitrile [10], indane-1,3-dione (and their dicyanovinyl analogues) [11], (thio) barbituric acid [12] and Meldrum's acid [13] have extensively been used as electron-withdrawing groups in push-pull molecules, while one of the highest $\mu\beta$ values were obtained for indane-1,3-dione and dicyanovinyl end-capped push-pull chromophores [14]. To the best of our knowledge, indane-1,3-dione-inspired cyclopenta[c] thiophen-4,6-dione (ThDione) has never been used in push-pull molecules as electron acceptor.

The aim of this research is to study the influence of various parameters affecting the ICT in model pyranylidene chromophores 1–15 by UV–Vis spectroscopy, electrochemistry, DFT calculation, and electric-field induced second harmonic (EFISH) experiments. The studied parameters are the nature of the intracyclic chalcogen atom (oxygen, sulfur and selenium), the position of substitution along the pyran ring (α- and γ-pyranylidenes), the length of the polyene π-conjugated bridge (ethylene, butadiene), and electron withdrawing nature of the acceptor (indane-1,3-dione, ThDione, N,N-dibutylbarbituric acid, N,N-dibutylthiobarbituric acid, and Meldrum's acid).

2. Results and discussion

2.1. Synthesis

Targeted push-pull derivatives 1–15 were prepared by Al_2O_3-catalyzed Knoevenagel condensations between (chalcogeno)pyr-anylidene aldehydes 16–20 and activated methylene derivatives in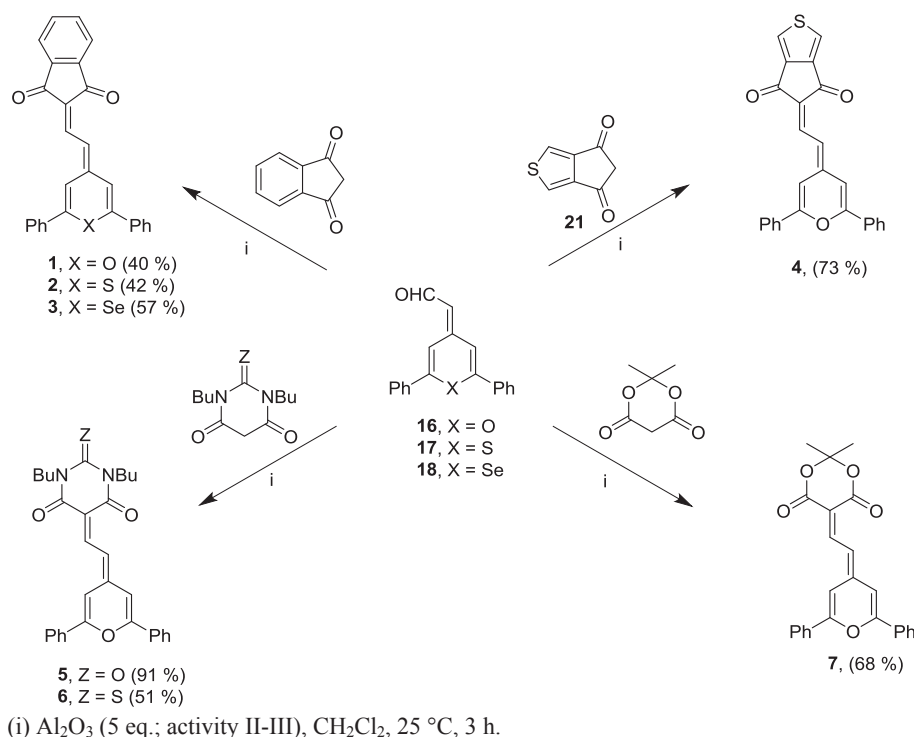 moderate to good yields (Schemes 1–3) [11a,15]. Pyranylidene aldehydes 16, 19, and 2016 and chalcogen analogues 17–18 [9a] were obtained according to literature procedures. Nonsymmetrical α-pyranylidene aldehyde 20 was obtained as an inseparable mixture of two stereoisomers. It should be noted that the E/Z ratio change for each product after purification by chromatography. Hence, the Knoevenagel condensation of 20 with activated methylene de-rivatives leads also to mixtures of two inseparable stereoisomers 13–15. For compounds 8–12 with extended π-conjugated linker, the central double bond exhibits exclusively (E)-configuration as proved by ^{1}H NMR spectroscopy with ^3J(H,H) equal to 12–13 Hz for the vinylic protons. The electron withdrawing moieties in 1–15 were represented by indane-1,3-dione, cyclopenta[c]thiophen-4,6-dione 21, N,N'-dibutyl(thio)barbituric[12b] and Meldrum's acid. The synthesis of ThDione 21 is outlined in Scheme 4. A treatment of commercially available thiophene-3,4-dicarboxylic acid with acetic anhydride afforded the corresponding anhydride [17] which further underwent Claisen condensation with ethyl acetoacetate (EAA) and subsequent acid-catalyzed decarboxylation. In this way, ThDione can conveniently be synthesized in 54% overall yield.

All new compounds are well soluble in THF, chloroform, and dichloromethane and were characterized by a variety of analytical techniques such as ^{1}H and ^{13}C NMR, IR, and HR-MS.

2.2. Electrochemistry

Electrochemical behavior of target compounds 1–15 was stud-ied by cyclic voltammetry in CH_2Cl_2 containing Bu_4NPF_6 electrolyte at a scan rate of 0.1 V/s. The working electrode was a glassy carbon disk, tungsten wire was used as the counter electrode, and a non-aqueous Ag/AgCl electrode was used as reference. The first oxida-tion/reduction peak potentials and their differences are listed in Table 1, representative CV diagrams of 4, 9, and 14 are shown in the SI.

The first oxidation/reduction potentials of 1–15 range from 0.28 to 0.77 and −1.43 to −1.18 V, respectively, and are obviously a

1, X = O (40 %)
2, X = S (42 %)
3, X = Se (57 %)

4, (73 %)

5, Z = O (91 %)
6, Z = S (51 %)

16, X = O
17, X = S
18, X = Se

7, (68 %)

(i) Al_2O_3 (5 eq.; activity II-III), CH_2Cl_2, 25 °C, 3 h.

Scheme 1. Synthesis of γ-pyranylidene push-pull derivatives **1–7**.
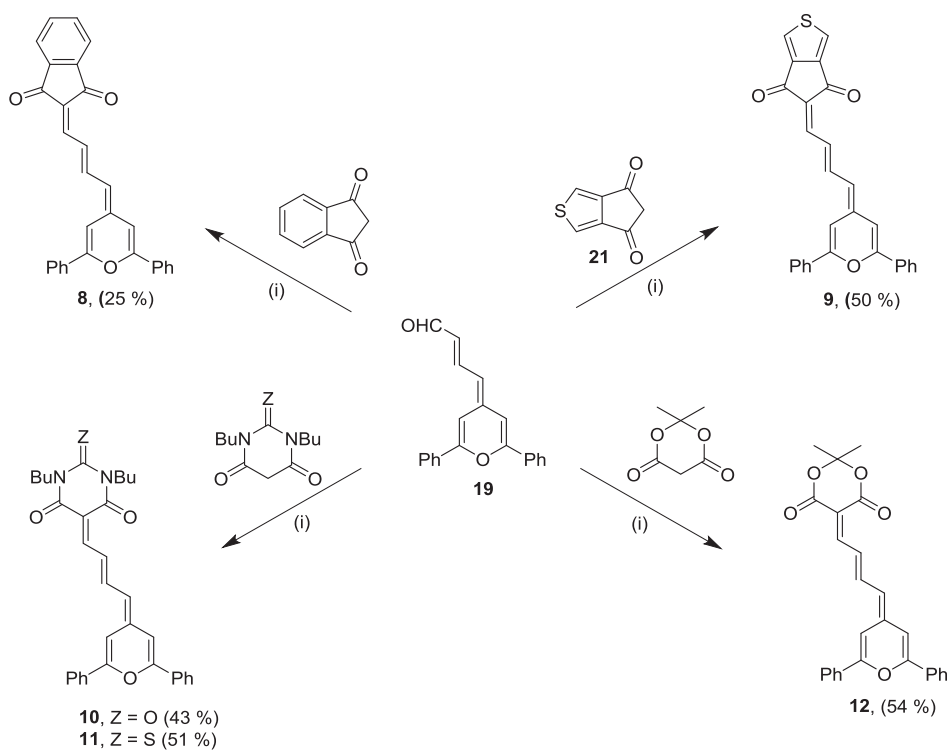
(i) Al$_2$O$_3$ (5 eq.; activity II-III), CH$_2$Cl$_2$, 25 °C, 3 h.

Scheme 2. Synthesis of γ-pyranylidene push-pull derivatives **8–12** with extended π-conjugated core.
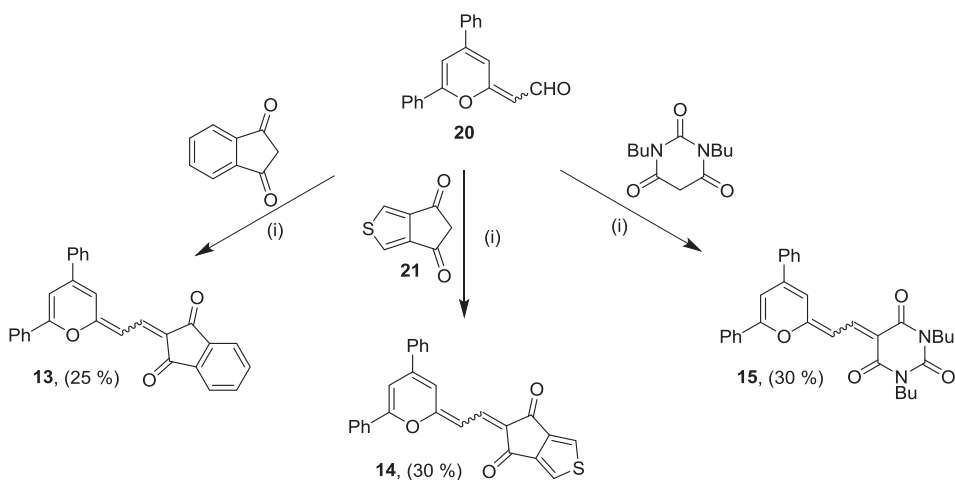
(i) Al$_2$O$_3$ (5 eq.; activity II-III), CH$_2$Cl$_2$, 25 °C, 24 h.

Scheme 3. Synthesis of α-pyranylidene push-pull derivatives **13–15**.
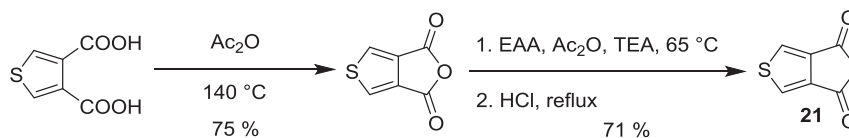
Scheme 4. Synthesis of ThDione **21**.

function of the chromophore structure. From the electrochemical data shown in Table 1 we can deduce the following general structure-property relationships:

- O→S or O→Se replacement in pyranylidene donors **1–3** slightly facilitated the first oxidation. For these compounds, reduction process is easier in the order O→S→Se. As a consequence a

Table 1
Electrochemical and optical data of chromophores 1−15.

Comp.	E_p^{ox1} [V][a]	$E_{1/2}^{red1}$ (ΔE) [V][a]	ΔE [V][b]	E_{HOMO} [eV][c]	E_{LUMO} [eV][c]	λ_{max} [nm][d]	ε [L.mmol.cm^{-1}][d]
1	0.50	−1.41 (80)	1.91	−5.30	−3.39	528/565	49.3/51.3
2	0.45	−1.29 (80)	1.74	−5.25	−3.51	556/596	52.2/46.5
3	0.46	−1.24 (80)	1.70	−5.26	−3.56	563/586(sh)	65.0/54.8
4	0.51	−1.34 (90)	1.85	−5.31	−3.46	538/575	78.1/89.4
5	0.66	−1.43 (87)	2.09	−5.46	−3.37	514/550	70.7/71.2
6	0.71	−1.31 (80)	2.02	−5.51	−3.49	537/575	59.1/86.5
7	0.77	−1.41 (90)	2.18	−5.57	−3.39	498/531	56.6/57.1
8	0.19	−1.30 (83)	1.49	−4.99	−3.50	599/654(sh)	64.5/44.2
9	0.19	−1.22 (88)	1.41	−4.99	−3.58	613/666	44.6/33.5
10	0.28	−1.30 (80)	1.58	−5.08	−3.50	589/639	68.0/48.9
11	0.29	−1.18 (92)	1.47	−5.09	−3.62	620/673	84.9/92.5
12	0.34	−1.30 (96)	1.64	−5.14	−3.50	576/623	85.7/65.1
13	0.39	−1.29 (80)	1.68	−5.19	−3.51	574/612(sh)	35.7/34.2
14	0.39	−1.27 (81)	1.66	−5.19	−3.53	619/656(sh)	34.2/19.9
15	0.58	−1.33 (80)	1.91	−5.38	−3.47	561/596	33.3/32.2

[a] All potentials are given versus ferrocene.
[b] $\Delta E = E_p^{ox1} - E_{1/2}^{red1}$. For the oxidation, E_p stand for $E_{1/2}$.
[c] $E_{HOMO} = -(E^{ox1} + 4.8)$, $E_{LUMO} = -(E^{red1} + 4.8)$.
[d] All spectra were recorded in CH_2Cl_2 solutions at room temperature at c = 1.0 to 2.0 × 10^{-5} M.

gradual narrowing of the electrochemical gap ΔE is observed ΔE (1.91→1.74→1.70).

- A systematic variation of the peripheral acceptor within the order of ThDione (**4**), indan-1,3-dione (**1**), thiobarbituric acid (**6**), barbituric acid (**5**), and Meldrum's acid (**7**) also affected both oxidation and reduction potentials and allowed tuning of the gap ΔE from 1.85 to 2.18 V. A similar trend can be seen within the series **8**−**12**.
- Considering the electrochemical data of structural analogues **1** and **4**−**7** and **8**−**12**, the newly developed ThDione and the thiobarbituric acid proved to be the strongest electron acceptors.
- In comparison to **1**, **4**−**7** (ΔE = 1.85−2.18 V), extension of the π-system by an additional olefinic unit as in **8**−**12** (ΔE = 1.41−1.64 V) reduced the electrochemical gap significantly.
- Shifting the position of the acceptor-terminated π-linker from γ to α position along the electron donating pyranylidene fragment narrowed the electrochemical gap within the limit of 0.18−0.23 V.
- Employing the aforementioned structural variations, the electrochemical gap in **1**−**15** can be tuned within the range of 2.18 to 1.41 V, with the lowest gap measured for chromophore **9** featuring ThDione acceptor and extended π-linker.

2.3. UV−vis spectroscopy

All target compounds are highly colored with the color ranging from orange, red to blue (Fig. 1). The UV−Vis electronic spectra of compounds **1**−**15** were recorded in dichloromethane and the results are given in Table 1. In general, three absorption bands were observed for chromophores **1**−**12**. The two more intense bands localized in the visible part of the spectra (λ_{max} = 498−673 nm) are
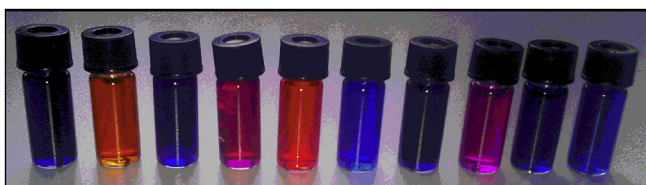
Fig. 1. Picture of solutions of **1**, **4-12** (from left to right) in DCM (c ~ 10^{-3} M).

attributed to the ICT (listed in Table 1). Representative spectra are shown in Fig. 2. Due to the presence of two stereoisomers, spectra of **13**−**15** feature six absorption bands. It should be noted that none of the studied compounds exhibited significant emission properties.

The positions of the CT absorption bands are clearly dependent on the structure of the chromophores. Concerning the CT bands, the following structure-property relationships can be highlighted:

- A replacement of pyranylidene donor by its chalcogen (sulfur and selenium) analogues leads to a bathochromic shift (e.g. **1**−**3**, Fig. 2a).
- A chalcogen exchange within the (thio)barbituric acceptor has a similar influence (e.g. **5**/**6** or **10**/**11**).
- The used acceptor moieties can be ordered according the position of the longest-wavelength absorption maxima in the following way (Fig. 2b): Meldrum's acid (**7** and **12**) < barbituric acid (**5** and **10**) < indane-1,3dione (**1** and **8**) < thiobarbituric acid (**6** and **11**) ≤ ThDione (**4** and **9**).
- Among the studied acceptors, novel ThDione and thiobarbituric acid impart the strongest ICT in the push-pull molecules.
- Compared to **1**, **4-7**, chromophores **8**−**12** with the extended π-linker showed red-shifted λ_{max} by about 100 nm (Fig. 2c).
- In accordance with the electrochemical observations, the absorption maxima of α-pyranylidenes **13**−**15** are red-shifted compared to γ-pyranylidene derivatives **1**, **4**−**5** (Fig. 2d).
- By varying the structure, the optical properties of **1**−**15** can be tuned within the range of 498(2.49)/673(1.84) nm(eV).

In term of relationships between optical and electrochemical properties, the general trend (except for compounds **3**, **11**, **14** and **15**) is the lower the HOMO-LUMO gap, the more red-shifted the absorption CT band.

2.4. EFISH experiments

Second-order non-linear properties were studied in CHCl$_3$ solution using the electric-field-induced second-harmonic generation technique (EFISH), which provides information about the scalar product $\mu\beta$ (2ω) of the vector component of the first hyperpolarisability tensor β and the dipole moment vector [18]. This product is derived according to equation (1) and considering γ_0(-2ω,ω,ω,0), the third-order term, as negligible for the push-pull

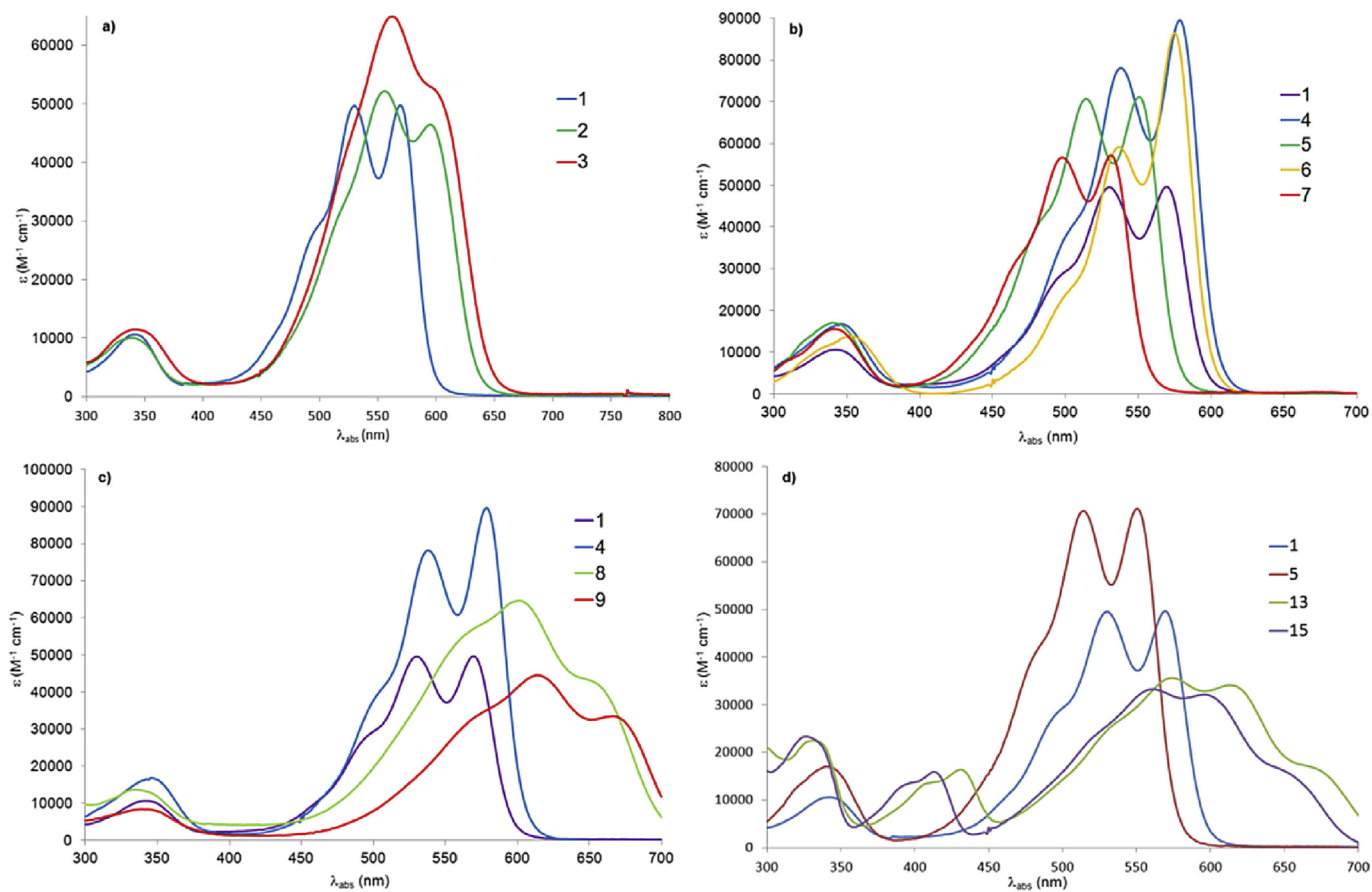**Fig. 2.** UV/Vis spectra of compounds a) **1**–**3** b) **1** and **4**–**7** c) **1**, **4**, **8**, and **9** d) **1**, **5**, **13**, and **15** in dichloromethane (c ~ 10^{-5} M).

compounds under consideration. This approximation is usually used for push-pull organic and organometallic molecules.

$$\gamma_{EFISH} = \mu\beta/5kT + \gamma_0(-2\omega,\omega,\omega,0) \quad (1)$$

Measurements were performed at 1907 nm, obtained from a Raman-shifted Nd:YAG laser source, which allowed us to work in conditions far from the resonance peaks of **1**–**15**. It should be noted that the sign and values of $\mu\beta$ depend on the "direction" of the transition implied in the NLO phenomena and on the direction of the ground-state dipole moment. When β and μ are parallel (antiparallel), positive (negative) maxima $\mu\beta$ values are reached. Except for compound **6**, all the $\mu\beta$ values (Table 2) are positive. In addition, this also implies that the ground and excited states are polarized in the same direction. The negative value observed for **6** indicates that zwitterionic arrangement of **6** is slightly predominant and a location in the C region of the Marder's plot [19]. This is in accordance with the value measured by Andreu and coworkers for a di-*tert*-butyl-substituted pyranylidene chromophore with N,N′-diethylthiobarbituric acid acceptor [7h]. Due to small positive $\mu\beta$ values measured for chromophores **5** and **15**, these compounds are also located close to the C region of the Marder's plot. As can be seen from the data gathered in Table 2, replacement of the oxygen atom by S or Se atom within the pyranylidene donor (compounds **1**–**3**) increases the $\mu\beta$ values despite the decrease of the ground state dipole moment value as observed previously [9c]. A chalcogen replacement (O→S) within the (thio)barbituric acceptors has also a significant impact on the NLO responses (e.g. **5**/**6** or **10**/**11**). In general, the effect of attaching various electron-withdrawing moieties mimics the trends seen for the linear optical properties

(Table 1), especially within the series **8**–**12** with the extended π-linker. Hence, the largest nonlinearities were measured for ThDione- and thiobarbituric acid-terminated chromophores **4**/**9** and **11**, respectively. From the data in Table 2 it is also clear that the length of the polyene π-conjugated bridge is the crucial parameter affecting the $\mu\beta$ values. Compared to ethylene analogues, a strong enhancement of the NLO response is observed for butadiene derivatives (e.g. **8** *vs* **1**, **9** *vs* **4**, **10** *vs* **5**, **11** *vs* **6**, and **12** *vs* **7**). α-Pyranylidene derivatives **13**–**15** exhibited $\mu\beta$ values within the same range as analogous γ-pyranylidene derivatives (e.g. **1** vs. **13**, **4** vs. **14**, and **5** vs. **15**).

2.5. DFT calculations

Spatial and electronic properties of all target chromophores **1**–**15** were investigated by DFT calculations using Gaussian W09 package [20]. Initial geometries were estimated by PM3 method implemented in ArgusLab [21] and these were subsequently optimized by the DFT B3LYP/6-311++G(2d,p) method. Energies of the HOMO and the LUMO, their differences, ground state dipole moments, and the second-order polarizabilities were calculated with the DFT B3LYP/6-311++G(2d,p) level. All calculated data are summarized in Table 2. The calculated energies of the HOMO/LUMO range from −5.89/−5.45 to −3.13/−2.87 eV. Both energies correlate very tightly with the experimental HOMO/LUMO levels obtained from the electrochemical measurements (see the SI). The calculated HOMO-LUMO gaps (ΔE^{DFT}) were found within the range from 2.97 to 2.38 eV (max. difference 0.6 eV) and showed even tighter correlation with the experimentally obtained electrochemical and

Table 2
DFT calculated properties and optical nonlinearities of chromophores **1**–**15**.

Comp.	E_{HOMO} [eV][a]	E_{LUMO} [eV][a]	ΔE^{DFT} [eV][b]	μ [D][c]	β (-2ω;ω,ω) [10^{-30} esu][d]	β (-2ω;ω,ω) [10^{-30} esu][e]	$\mu\beta$ [10^{-48} esu][f]
1	−5.72	−2.93	2.79	8.58	34.50	14.00	170
2	−5.66	−3.03	2.63	7.60	57.40	32.60	250
3	−5.65	−3.09	2.56	7.11	78.10	42.70	230
4	−5.73	−3.00	2.73	9.31	56.10	27.50	430
5	−5.79	−2.90	2.89	11.64	19.50	17.80	50
6	−5.83	−3.05	2.78	14.43	60.40	59.90	−70
7	−5.89	−2.92	2.97	10.69	10.80	6.81	130
8	−5.45	−3.02	2.43	11.31	181.00	76.10	1050
9	−5.46	−3.08	2.38	12.16	233.00	103.00	1200
10	−5.51	−2.99	2.52	14.52	55.80	16.90	1300
11	−5.55	−3.13	2.42	17.73	39.10	46.40	1500
12	−5.57	−3.00	2.57	13.69	51.00	20.50	900
13E	−5.63	−2.89	2.74	9.62	43.20	13.00	180
13Z	−5.61	−2.99	2.62	9.58	39.30	8.94	
14E	−5.64	−2.94	2.70	10.37	65.90	25.90	230
14Z	−5.63	−3.04	2.59	10.32	61.90	22.30	
15E	−5.70	−2.87	2.83	12.61	9.84	16.70	70
15Z	−5.68	−2.97	2.71	12.58	15.40	21.30	

[a] DFT calculated energies of the HOMO/LUMO in CH_2Cl_2 (PCM).
[b] $E_{HOMO} - E_{LUMO}$.
[c] DFT calculated ground state dipole moment in CH_2Cl_2.
[d] Calculated second-order polarizability in $CHCl_3$ at 1907 nm.
[e] Calculated second-order polarizability in vacuum at 1907 nm.
[f] $\mu\beta$ (2ω) at 1907 nm in $CHCl_3$. Molecular concentrations used for the measurements were in the range 10^{-3} to 10^{-2} M. $\mu\beta \pm 10\%$.

optical gaps (see the SI). Hence, the used DFT method can be considered as a reasonable tool for the description of electronic properties of **1**–**15**. As a consequence, very similar trends as deduced from the electrochemical data and positions of the longest-wavelength absorption maxima can also be seen from the calculated data. Namely, ΔE^{DFT} depends primarily on the π-linker extension, character of the acceptor attached, chalcogen atom involved in the pyranylidene donor as well as in the (thio)barbituric acceptor, substitution of the pyranylidene fragment (γ and α), and also by the double bond conformation. Length of the π-linker affected the calculated HOMO and LUMO energies and their differences most significantly (e.g. **1** *vs* **8**; **4** *vs* **9**; **5** *vs* **10**; **6** *vs* **11** or **7** *vs* **12**, Table 2). Replacing the peripheral acceptor affected the ΔE^{DFT} within a limit of about 0.2–0.3 eV (e.g. **1**, **4**–**7** or **8**–**12**). Within the particular three subseries, ThDione-terminated chromophores **4**, **9**, and **14** showed the lowest HOMO-LUMO gaps. The increased polarizability and molecular weight of the chalcogen atom involved in pyranylidene fragment (O→S→Se) lowered ΔE^{DFT} in **1**–**3**. In general, Z-isomers of α-pyranylidenes **13**–**15** possess lower calculated total energies and thus can be considered as energetically preferred. In Z-configured **13**–**15** is the pyranylidene oxygen atom in a close proximity of the adjacent olefinic hydrogen, which may imply higher stabilization of this isomer via H-bonding. Hence, narrowed HOMO-LUMO gaps were calculated for Z isomers. In accordance with the electrochemical measurements, the α-substituted pyranylidene chromophores **13**–**15** showed lower gaps when compared to γ-pyranylidenes **1**, **4**, and **5**.

Representative visualizations of the HOMO and LUMO localizations for chromophores **4**, **8**, and (Z)-**15** are depicted in Fig. 3. For complete listing see the SI. As a general trend, the HOMO as well the HOMO−1 is localized on the π-linker connecting both pyranylidene fragment and the given acceptor. Both orbitals are also partially spread over β- and γ-carbon atoms of the pyrane ring. The LUMO in **4** and **8** is localized not on the acceptor but rather on the π-linker and α-carbon atoms of the pyrane, whereas the LUMO+1 is completely localized on the diphenylpyran moiety. This is conversely to α-pyranylidene derivatives e.g. (Z)-**15**. Despite these counterintuitive results, these observations are in accordance with those observed for other proaromatic pyranylidene chromophores
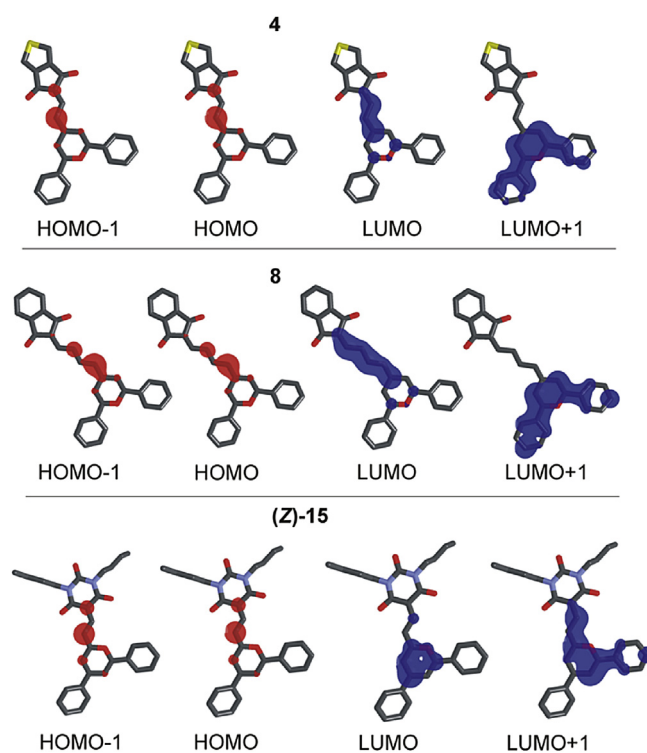
Fig. 3. Localization of frontier molecular orbitals in representative chromophores **4**, **8**, and (Z)-**15**.

[7g] and imply that **1**–**15** are strongly polarized with the pyranylidene donor adopting positively charged pyrylium character. The calculated ground state dipole moments of **1**–**15** (Table 2) range from about 7 to 18 D with the highest ones computed for chromophores **6** and **11** bearing an N,N-dibutyl-2-thiobarbituric acceptor. On the contrary, chromophores **1**–**3**, **8**, and **13** with attached indane-1,3-dione showed the lowest values. Molecular second order optical nonlinearities β were calculated at 1907 nm

either in vacuum or CHCl$_3$. The computed β (-2ω;ω,ω) values are given in Table 2. Generally higher β coefficients were calculated in CHCl$_3$ than in vacuum. Within the particular subseries **1**–**3**, **1**–**7**, **8**–**12**, and **13**–**15** the calculated second-order polarizabilities mimic the trends seen for the experimentally obtained $\mu\beta$ values. When going from **1** to **3**, the chalcogen replacement within the pyranylidene fragment slightly improved the optical nonlinearities. Similarly to EFISHG measured $\mu\beta$ values, the largest optical non-linearities were calculated for chromophores **8**–**12** with the extended butadiene π-conjugated bridge. Hence, the length of the π-linker seems to be the most crucial factor affecting optical non-linearities of target compounds. On the contrary, when going from **6** to **11** a slight decrease of the calculated β coefficients has been observed. The highest β values were calculated for extended chromophores **8**–**12** and ThDione seems to be the most suited acceptor moiety delivering the highest calculated nonlinearity in **9** ($\beta = 233/103 \times 10^{-30}$ esu).

3. Conclusion

Starting from three types of pyranylidene aldehydes and their chalcogen analogues, we have prepared fifteen new push-pull D-π-A compounds **1**–**15**. Property tuning has been achieved by variation of the acceptor moiety, extension of the π-linker, chalcogen replacement within the pyranylidene as well as in (thio)barbituric fragments, and substitution of the pyranylidene donor. These structural changes allowed tuning of the electrochemically measured HOMO-LUMO gap within the range of 2.18 to 1.41 eV, the optical gap can be tuned from 498(2.49) to 673(1.84) nm (eV). The employed electron withdrawing moieties include novel ThDione, *N*,*N'*-dibutyl(thio)barbituric acids, indane-1,3-dione, and Meldrum's acid. ThDione and thiobarbituric acid impart the strongest ICT into proaromatic systems and can be considered as strongest acceptors within the studied series. Thorough structure-property relationships were elucidated from both experimental as well as calculated data. Both approaches suggest charge-separated (zwitterionic) ground-state character of **1**–**15** as evidenced by the electrochemistry, absorption spectra, and DFT. The optical nonlinearities of **1**–**15** measured by EFISH experiments showed trends in accordance to the ICT efficiency. Namely, the highest NLO responses were observed for the chromophores bearing ThDione and thiobarbituric acceptors and extended π-system. In view of the current interest push-pull molecules with enhanced ICT, this fundamental research provides the impetus for further application of proaromatic pyranylidene-derived chromophores and novel ThDione acceptor in molecular electronics.

4. Experimental section

4.1. General

Reagent-grade reagents and solvents were purchased from Sigma-Aldrich, Acros, TCI Europe and Alfa Aesar and used as received. Pyranylidene aldehyde and their chalcogen analogues were obtained according to reported procedures [9a,16]. Column chromatography was performed with silica gel 60 (Macherey-Nagel, particule size 0.040–0.063 nm, 230–400 mesh) and indicated solvent. TLC was conducted with aluminum sheets coated with silica gel 60 F254 (Merck or Macherey Nagel) with visualization by a UV lamp (254 and 360 nm). NMR spectra were acquired at room temperature on a Bruker AC-300, AVANCE 400 or AVANCE 500 spectrometer. Chemical shifts are given in parts per million relative to TMS (^{1}H, 0.0 ppm) and CDCl$_3$ (^{13}C, 77.0 ppm). Acidic impurities in CDCl$_3$ were removed by treatment with anhydrous K$_2$CO$_3$. For compounds **13-15**, identification of the two isomers is

based on NOESY analysis performed on similar push-pull α-pyranylidene push-pull derivatives (unpublished results). High resolution mass analyses were performed at the "Centre Régional de Mesures Physiques de l'Ouest" (CRMPO, University of Rennes1) using a Bruker MicroTOF-Q II apparatus. High-resolution MALDI MS spectra were recorded with an LTQ Orbitrap XL MALDI mass spectrometer (Thermo Fisher Scientific) equipped with a nitrogen UV laser (337 nm, 60 Hz). The matrix was 2,5-dihydroxybenzoic acid (DHB). More details concerning MALDI HRMS analysis are given elsewhere [11a]. Elemental analyses were performed with an EA 1108 Fisons instrument. IR spectra were recorded on either a Perkin–Elmer spectrum1000 FTIR using KBr plates or Nicolet 6700 with single-bounce diamond ATR. UV/vis spectra were recorded with a UVIKON xm SECOMAM spectrometer using standard 1 cm quartz cells. Cyclic voltammetric experiments were performed in a three electrodes cell using a potentiostat (Autolab PGSTAT 12) driven by the GPES software. The working electrode consisted of a vitreous carbon disk. The Ag/Ag$^+$ reference electrode was separated from the analyte by a CH$_2$Cl$_2$–[NBu$_4$][PF$_6$] bridge. All the potentials are quoted against the ferrocene–ferrocenium couple; ferrocene was added as an internal standard at the end of each experiment.

4.2. General procedure for the synthesis of push-pull derivatives

The corresponding activated methylene derivative (1.00 mmol) and the corresponding pyranylidene aldehyde (1.00 mmol) were dissolved in CH$_2$Cl$_2$ (5 mL), Al$_2$O$_3$ activity II–III (510 mg, 5.00 mmol) was added and the reaction was stirred at room temperature for 3 h (24 h for **13**–**15**). Al$_2$O$_3$ was then filtered off, the solvent was evaporated *in vacuo* and the crude product was purified by column chromatography over SiO$_2$.

4.3. 2-[2-(2,6-Diphenyl-pyran-4-ylidene)-ethylidene]-indan-1,3-dione (1)

Purified by column chromatography (CH$_2$Cl$_2$/petroleum ether, 2:1). Dark solid (160 mg, 40%). Mp > 260 °C. ^{1}H NMR (300 MHz, CDCl$_3$): δ = 6.97 (d, 1H, J = 1.5 Hz), 7.48 (s, 2H), 7.52–7.57 (m, 6H), 7.65–7.68 (m, 2H), 7.83–7.88 (m, 4H), 8.08 (d, 1H, J = 13.8 Hz) ppm. ^{13}C NMR (75 MHz, CDCl$_3$): δ = 103.5 (CH), 110.4 (CH), 111.8 (CH), 120.3 (C), 121.8 (CH), 122.1 (CH), 125.0 (CH), 125.8 (CH), 129.1 (CH), 131.2 (CH), 131.3 (CH), 131.4 (C), 131.6 (C), 133.7 (CH), 133.8 (CH), 138.8 (CH), 140.5 (C), 142.0 (C), 149.8 (C), 157.8 (C), 157.6 (C), 191.6 (C), 191.9 (C) ppm. IR (KBr): ν = 2922 (C-H), 1699 (C=O), 1654 (C=C), 1492 (C-O), 1451, 1208, 1152, 941, 728 (=C-H), 678 (=C-H) cm^{-1}. HRMS (ESI/ASAP) *m/z* calculated for C$_{28}$H$_{19}$O$_3$ [M+H]$^+$ 403.1329, found 403.1321.

4.4. 2-[2-(2,6-Diphenyl-thiopyran-4-ylidene)-ethylidene]-indan-1,3-dione (2)

Purified by column chromatography (ethyl acetate/petroleum ether, 1:1). Dark solid (177 mg, 42%). Mp > 260 °C. ^{1}H NMR (300 MHz, CDCl$_3$): δ = 7.31 (s, 1H), 7.48–7.53 (m, 6H), 7.63–7.72 (m, 7H), 7.84–7.86 (m, 3H), 8.11 (d, 1H, J = 13.8 Hz) ppm. ^{13}C NMR (75 MHz, CDCl$_3$): δ = 118.4 (CH), 119.7 (CH), 121.3 (C), 121.9 (CH), 122.2 (CH), 126.5 (CH), 126.8 (CH), 127.1 (CH), 129.3 (CH), 130.5 (CH), 130.6 (CH), 133.8 (CH), 134.0 (CH), 136.4 (C), 136.7 (C), 137.8 (CH), 140.6 (C), 142.2 (C), 145.5 (C), 147.0 (C), 150.5 (C), 191.3 (C), 191.7 (C) ppm. IR (KBr): ν = 1661 (C=O), 1509 (C-S), 1352, 1324, 1228, 986, 751 (=C-H) cm^{-1}. HRMS (ESI/ASAP) *m/z* calculated for C$_{28}$H$_{18}$O$_2$NaS [M+Na]$^+$ 441.0925, found 441.0927.

4.5. 2-[2-(2,6-Diphenyl-selenopyran-4-ylidene)-ethylidene]-indan-1,3-dione (3)

Purified by column chromatography (ethyl acetate/petroleum ether, 1:1). Dark solid (264 mg, 57%). Mp > 260 °C. ^{1}H NMR (300 MHz, CDCl$_3$): δ = 7.37 (s, 1H), 7.48−7.52 (m, 6H), 7.58−7.63 (m, 4H), 7.68−7.71 (m, 2H), 7.82−7.90 (m, 4H), 8.17 (d, 1H, J = 13.8 Hz) ppm. ^{13}C NMR (75 MHz, CDCl$_3$): δ = 120.5 (CH), 121.7 (CH), 122.1 (C), 122.2 (CH), 122.4 (CH), 126.5 (CH), 126.9 (CH), 128.4 (CH), 129.4 (CH), 130.3 (CH), 130.4 (CH), 134.0 (CH), 134.1 (CH), 137.7 (CH), 138.3 (C), 138.6 (C), 140.7 (C), 142.3 (C), 148.0 (C), 148.6 (C), 150.9 (C), 191.3 (C), 191.7 (C) ppm. IR (KBr): ν = 1663 (C=O), 1529 (C=C), 1351, 1209, 729 (=C-H) cm^{-1}. HRMS (ESI/ASAP) m/z calculated for C$_{28}$H$_{18}$O$_2$Na^{80}Se [M+Na]$^+$ 489.0370, found 489.0370.

4.6. 5-(2-(2,6-Diphenyl-4H-pyran-4-ylidene)ethylidene)-4H-cyclopenta[c]thiophene-4,6(5H)-dione (4)

Purified by column chromatography (ethyl acetate/hexane, 1:1). Dark solid (300 mg, 73%). Mp 300−305 °C. ^{1}H NMR (500 MHz, CDCl$_3$): δ = 7.00 (d, 1H, J = 1.5 Hz), 7.49 (d, 2H, J = 13.5 Hz), 7.52−7.55 (m, 6H), 7.74−7.76 (m, 2H), 7.85−7.87 (m, 2H), 7.92−7.94 (m, 2H), 8.05 (d, 1H, J = 13.5 Hz) ppm. ^{13}C NMR (125 MHz, CDCl$_3$): δ = 104.0 (CH), 110.9 (CH), 112.1 (CH), 123.0 (CH), 123.3 (CH), 125.8 (CH), 126.1 (CH), 128.5 (C), 129.4 (CH), 129.5 (CH), 131.4 (C), 131.5 (CH), 131.6 (CH), 131.7 (C), 140.6 (CH), 146.5 (C), 147.7 (C), 150.8 (C), 158.4 (C), 158.6 (C), 184.9 (C), 185.5 (C) ppm. IR (KBr): ν = 2953 (C-H), 1651 (C=O), 1455 (C-O), 1159 cm^{-1}. HRMS (MALDI) m/z calculated for C$_{26}$H$_{17}$O$_3$S [M+H]$^+$ 409.0898, found 409.0901. Anal. Calcd for C$_{26}$H$_{16}$O$_3$S: C, 76.45; H, 3.95; S, 7.85. Found: C, 75.98; H, 3.94; S, 8.20.

4.7. 1,3-Dibutyl-5-(2-(2,6-diphenyl-4H-pyran-4-ylidene)ethylidene)pyrimidine-2,4,6(1H,3H,5H)-trione. (5)

Purified by column chromatography (CH$_2$Cl$_2$/hexane, 3:1). Dark solid (451 mg, 91%). Mp 281−284 °C. ^{1}H NMR (400 MHz, CDCl$_3$): δ = 0.93−0.97 (m, 6H), 1.35−1.42 (m, 4H), 1.59−1.66 (m,4H), 3.91−3.97 (m, 4H), 6.99 (s, 1H), 7.51−7.54 (m, 7H), 7.68 (d, 1H, J = 14.0 Hz), 7.81−7.84 (m, 2H), 7.89−7.92 (m, 2H), 8.65 (d, 1H, J = 14.0 Hz) ppm. ^{13}C NMR (125 MHz, CDCl$_3$): δ = 14.0 (CH$_3$), 20.5 (CH$_2$), 20.6 (CH$_2$), 30.5 (CH$_2$), 30.6 (CH$_2$), 41.2 (CH$_2$), 41.8 (CH$_2$), 104.2 (CH), 105.5 (C), 111.9 (CH), 113.2 (CH), 125.8 (CH), 126.1 (CH), 129.4 (CH), 129.5 (CH), 131.2 (C), 131.4 (C), 131.8 (CH), 131.9 (CH), 149.2 (CH), 151.7 (C), 152.9 (C), 159.0 (C), 159.2 (C), 163.0 (C), 163.8 (C) ppm. IR (KBr): 1653 (C=O), 1538 (C=C), 1477 (C-O), 1223 cm^{-1}. HRMS (MALDI) m/z calculated for C$_{31}$H$_{33}$N$_2$O$_4$ [M+H]$^+$ 497.2434, found 497.2455. Anal. Calcd for C$_{31}$H$_{32}$N$_2$O$_4$: C, 74.98; H, 6.50; N, 5.64. Found: C, 74.81; H, 6.47; N, 5.60.

4.8. 1,3-Dibutyl-5-(2-(2,6-diphenyl-4H-pyran-4-ylidene)ethylidene)-2-thioxodihydropyrimidine-4,6(1H,5H)-dione. (6)

Purified by column chromatography (CH$_2$Cl$_2$/hexane, 3:1). Dark solid (261 mg, 51%). Mp 294−297 °C. ^{1}H NMR (500 MHz, CDCl$_3$): δ = 0.95−0.97 (m, 6H), 1.39−1.43 (m, 4H), 1.71−1.73 (m, 4H), 4.47−4.8 (m, 4H), 7.08 (s, 1H), 7.24 (s, 1H), 7.54−7.60 (m, 6H), 7.77 (d, 1H, J = 14.0 Hz), 7.85 (d, 2H, J = 6.2 Hz), 7.93 (d, 2H, J = 6.2 Hz), 8.67 (d, 1H, J = 14.0 Hz) ppm. ^{13}C NMR (125 MHz, CDCl$_3$): δ = 14.1 (CH$_3$), 20.5 (CH$_2$), 20.6 (CH$_2$), 29.4 (CH$_2$), 29.9 (CH$_2$), 47.8 (CH$_2$), 48.3 (CH$_2$), 104.9 (CH), 106.0 (C), 111.7 (CH), 114.4 (CH), 126.0 (CH), 126.3 (CH), 129.5 (CH), 129.6 (CH), 130.9 (C), 131.0 (C), 131.1 (CH), 132.2 (CH), 150.0 (CH), 154.6 (C), 160.0 (C), 160.4 (C), 161.2 (C), 162.5 (C), 179.1 (C) ppm. IR (ATR): ν = 1638 (C=O), 1482 (C-O), 1372, 1342, 1225 (C=S), 1180, 1120, 927, 766 (=C-H), 682 (=C-H) cm^{-1}. HRMS

(MALDI) m/z calculated for C$_{31}$H$_{33}$N$_2$O$_3$S [M+H]$^+$ 513.2206, found 513.2211. Anal. Calcd for C$_{31}$H$_{32}$N$_2$O$_3$S: C, 72.63; H, 6.29; N, 5.46; S, 6.25. Found: C, 72.93; H, 6.67; N, 6.60; S, 6.48.

4.9. 5-(2-(2,6-Diphenyl-4H-pyran-4-ylidene)ethylidene)-2,2-dimethyl-1,3-dioxane-4,6-dione (7)

Purified by column chromatography (ethyl acetate/hexane, 1:1). Dark solid (272 mg, 68%). Mp: 255−257 °C. ^{1}H NMR (500 MHz, CDCl$_3$): δ = 1.72 (s,6H), 6.99 (d, 1H, J = 1.7 Hz), 7.38 (d, 1H, J = 14.0 Hz), 7.45 (d, 1H, J = 1.7 Hz), 7.50−7.55 (m, 6H), 7.82−7.84 (m, 2H), 7.88−7.91 (m, 2H), 8.56 (d, 1H, J = 14.0 Hz) ppm. ^{13}C NMR (125 MHz, CDCl$_3$): δ = 27.4 (CH$_3$), 99.7 (C), 103.8 (C), 104.1 (CH), 110.9 (CH), 112.8 (CH), 125.9 (CH), 126.1 (CH), 129.4 (CH), 129.5 (CH), 131.0 (C), 131.2 (C), 131.9 (CH), 149.9 (CH), 153.1 (C), 159.3 (C), 159.6 (C), 162.9 (C), 165.4 (C) ppm. IR (ATR): ν = 1690 (C=O), 1648 (C=C), 1524, 1484 (C-O), 1365, 1235, 1157, 945, 884, 765 (=C-H), 682 (=C-H) cm^{-1}. HRMS (MALDI) m/z calculated for C$_{25}$H$_{20}$O$_5$ M$^+$ 400.1305, found 400.1317. Anal. Calcd for C$_{25}$H$_{20}$O$_5$: C, 74.99; H, 5.03; Found: C, 74.91; H, 5.19.

4.10. 2-[4-(2,6-Diphenyl-pyran-4-ylidene)-but-2-enylidene]-indan-1,3-dione (8)

Purified by column chromatography (CH$_2$Cl$_2$/petroleum ether, 2:1). Dark solid (107 mg, 25%). Mp > 260 °C. ^{1}H NMR (300 MHz, CDCl$_3$): δ = 6.08 (d, 1H, 12 Hz), 6.62 (d, 1H, J = 1.5 Hz), 7.03 (d, 1H, J = 1.2 Hz), 7.47−7.53 (m, 6H), 7.58 (d, 2H, J = 12.0 Hz), 7.64−7.67 (m, 2H), 7.72 (s, 1H), 7.77−7.83 (m, 6H) ppm. ^{13}C NMR (75 MHz, CDCl$_3$): δ = 103.1 (CH), 109.3 (CH), 115.9 (CH), 122.0 (CH), 122.2 (CH), 122.9 (CH), 123.8 (C), 125.1 (CH), 125.3 (CH), 128.9 (CH), 129.0 (CH), 130.5 (CH), 130.6 (CH), 131.8 (C), 132.0 (C), 133.9 (CH), 134.1 (CH), 140.8 (C), 141.3 (C), 142.1 (C), 145.4 (CH), 148.5 (CH), 155.6 (C), 155.8 (C), 191.0 (C), 191.2 (C) ppm. IR (KBr): ν = 2342 (C-H), 1669 (C=O), 1597, 1540, 1371, 1330, 1176, 1023, 937, 728 (=C-H), 670 (=C-H) cm^{-1}. HRMS (ESI/ASAP) m/z calculated for C$_{30}$H$_{21}$O$_3$ [M+H]$^+$ 429.1485, found 429.1480.

4.11. (E)-5-(4-(2,6-Diphenyl-4H-pyran-4-ylidene)but-2-en-1-ylidene)-4H-cyclopenta[c]thiophene-4,6(5H)-dione (9)

Purified by column chromatography (ethyl acetate/hexane, 1:1). Dark solid (217 mg, 50%). Mp: 275−278 °C. ^{1}H NMR (500 MHz, CDCl$_3$): δ = 6.09 (d, 1H, J = 12.5 Hz), 6.65 (d, 1H, J = 1.5 Hz), 7.05 (s, 1H), 7.48−7.59 (m, 8H), 7.72−7.81 (m, 7H) ppm. ^{13}C NMR (125 MHz, CDCl$_3$): δ = 103.5 (CH), 109.7 (CH), 116.3 (CH), 123.5 (CH), 123.6 (CH), 123.9 (CH), 125.3 (CH), 125.4 (CH), 125.6 (CH), 129.2 (CH), 129.3 (CH), 130.8 (CH), 130.9 (CH), 131.0 (CH), 131.9 (C), 132.1 (C), 142.4 (C), 146.6 (C), 147.2 (C), 147.3 (CH), 147.6 (C), 149.3 (CH), 156.2 (C), 156.3 (C), 184.4 (C), 184.8 (C) ppm. IR (KBr): 2953 (C-H), 1644 (C=O), 1507 (C=C), 1488 (C-O), 1228 cm^{-1}. HRMS (MALDI) m/z calculated for C$_{28}$H$_{19}$O$_3$S [M+H]$^+$ 435.1055, found 435.1069. Anal. Calcd for C$_{28}$H$_{18}$O$_3$S: C, 77.40; H, 4.18; S, 7.38. Found: C, 77.76; H, 4.47; S, 7.40.

4.12. (E)-1,3-Dibutyl-5-(4-(2,6-diphenyl-4H-pyran-4-ylidene)but-2-en-1-ylidene)pyrimidine-2,4,6(1H,3H,5H)-trione. (10)

Purified by column chromatography (CH$_2$Cl$_2$/hexane, 3:1). Dark solid (224 mg, 43%). Mp: 216−219 °C. ^{1}H NMR (400 MHz, CDCl$_3$): δ = 0.91−0.96 (m, 6H), 1.34−1.43 (m, 4H), 1.58−1.62 (m, 4H), 3.90−3.95 (m, 4H), 6.07 (d, 1H, J = 12.0 Hz), 6.68 (d, 1H, J = 1.6 Hz), 7.11 (d, 1H, J = 1.6 Hz), 7.48−7.53 (m, 6H), 7.68 (dd, 1H, J_1 = 13.2 Hz, J_2 = 12.0 Hz), 7.81−7.87 (m, 4H), 7.92 (dd, 1H, J_1 = 13.2 Hz, J_2 = 12.0 Hz), 8.11 (d, 1H, J = 12.0 Hz) ppm. ^{13}C NMR (125 MHz, CDCl$_3$): δ = 14.0 (CH$_3$), 20.4 (CH$_2$), 20.5 (CH$_2$), 30.5 (CH$_2$), 30.6 (CH$_2$),

41.2 (CH$_2$), 41.8 (CH$_2$), 104.0 (CH), 108.3 (C), 109.8 (CH), 116.1 (CH), 125.0 (CH), 125.5 (CH), 125.6 (CH), 129.2 (CH), 129.3 (CH), 131.0 (CH), 131.1(CH), 131.8(C), 132.0 (C), 143.8 (C), 151.7 (C), 151.9 (CH), 156.7(C), 156.9 (CH), 162.5 (C), 163.2 (C) ppm. IR (KBr): 1647 (C=O), 1484 (C-O), 1396, 1174 cm^{-1}. HRMS (MALDI) m/z calculated for C$_{33}$H$_{35}$N$_2$O$_4$ [M+H]$^+$ 523.2591, found 523.2593. Anal. Calcd for C$_{33}$H$_{34}$N$_2$O$_4$: C, 75.84; H, 6.56; N, 5.36. Found: C, 76.12; H, 6.86; N, 5.10.

4.13. (E)-1,3-Dibutyl-5-(4-(2,6-diphenyl-4H-pyran-4-ylidene)but-2-en-1-ylidene)-2-thioxodihydropyrimidine-4,6(1H,5H)-dione (11)

Purified by column chromatography (CH$_2$Cl$_2$/hexane, 3:1). Dark solid (274 mg, 51%). Mp: 258–260 °C. ^{1}H NMR (400 MHz, CDCl$_3$): δ = 0.93−0.97 (m, 6H), 1.35−1.42 (m, 4H), 1.65−1.74 (m, 4H), 4.42−4.46 (m, 4H), 6.11 (d, 1H, J = 12.0 Hz), 6.73 (d, 1H, J = 1.6 Hz), 7.15 (d, 1H, J = 1.6 Hz), 7.49−7.55 (m, 6H), 7.72 (dd, 1H, J_1 = 13.0 Hz, J_2 = 12.0 Hz), 7.81−7.87 (m, 4H), 7.94 (dd, 1H, J_1 = 13.0 Hz, J_2 = 12.0 Hz), 8.01 (d, 1H, J = 13.0 Hz) ppm. ^{13}C NMR (125 MHz, CDCl$_3$): δ = 14.1 (CH$_3$), 20.4 (CH$_2$), 20.5 (CH$_2$), 29.3 (CH$_2$), 29.4 (CH$_2$), 47.8 (CH$_2$), 48.2 (CH$_2$), 103.9 (CH), 108.3 (C), 110.1 (CH), 116.7 (CH), 125.5 (CH), 125.6 (CH), 129.8 (CH), 126.2 (CH), 129.3 (CH), 129.4 (CH), 131.4 (CH), 131.5 (CH), 131.6 (C), 145.7 (C), 153.2(CH), 157.5 (C), 157.6 (CH), 157.7 (C), 160.7 (C), 161.8 (C) ppm. IR (ATR): ν = 1692 (C=O), 1532 (C=C), 1468 (C-O), 1363, 1281 (C=S), 1144, 934, 763 (=C-H), 681 (=C-H) cm^{-1}. HRMS (DHB) m/z calculated for C$_{33}$H$_{35}$N$_2$O$_3$S [M+H]$^+$ 539.2362, found 539.2366. Anal. Calcd for C$_{33}$H$_{34}$N$_2$O$_3$S: C, 73.58; H, 6.36; N 5.20; S, 5.95. Found: C, 73.75; H, 6.46; N, 5.57; S, 6.13.

4.14. (E)-5-(4-(2,6-Diphenyl-4H-pyran-4-ylidene)but-2-en-1-ylidene)-2,2-dimethyl-1,3-dioxane-4,6-dione (12)

Purified by column chromatography (ethyl acetate/hexane, 1:1). Dark solid (230 mg, 54%). Mp: 238−241 °C. ^{1}H NMR (400 MHz, CDCl$_3$): δ = 1.71 (s, 6H), 6.07 (d, 1H, J = 13.0 Hz), 6.68 (d, 1H, J = 1.8 Hz), 7.09 (d, 1H, J = 1.8 Hz), 7.49−7.53 (m, 6H), 7.63−7.66 (m, 2H), 7.79−7.86 (m, 4H), 8.06 (d, 1H, J = 12.0 Hz) ppm. ^{13}C NMR (100 MHz, CDCl$_3$): δ = 27.9 (CH$_3$), 103.0 (C), 103.5 (CH), 104.0 (C), 109.8 (CH), 115.7 (CH), 124.2 (CH), 125.5 (CH), 125.6 (CH), 129.2 (CH), 129.3 (CH), 131.1 (CH), 131.2 (CH), 131.7 (C), 131.9 (C), 144.5 (C), 151.9 (CH), 157.0 (C), 157.1 (C), 157.7 (CH), 162.3 (C), 162.4 (C) ppm. IR (ATR): ν = 1648 (C=O), 1471 (C=C), 1381 (C-O), 1171, 1120, 937, 916, 781, 763 (=C-H), 677 (=C-H) cm^{-1}. HRMS (DHB) m/z calculated for C$_{27}$H$_{22}$O$_5$ M$^+$ 426.1462, found 426.1467. Anal. Calcd for C$_{27}$H$_{22}$O$_5$: C, 76.04; H, 5.20. Found: C, 75.82; H, 5.21.

4.15. 2-[2-(4,6-Diphenyl-pyran-2-ylidene)-ethylidene]-indan-1,3-dione (13)

The title compound, as a mixture of two (E/Z) isomers with 1:2 ratio (based on integration of ethylenic protons) was obtained following the general procedure and was purified by column chromatography (CH$_2$Cl$_2$/petroleum ether, 2:1). Dark solid (99 mg, 25%). Mp > 260 °C. ^{1}H NMR (major isomer, 300 MHz, CDCl$_3$): δ = 6.97 (d, 1H, J = 0.6 Hz), 6.99 (d, 1H, J = 0.6 Hz), 7.35 (d, 1H, J = 13.5 Hz), 7.55−7.60 (m, 6H), 7.67−7.71 (m, 4H), 7.85−7.87 (m, 2H), 7.95−7.98 (m, 2H), 8.26 (d, 1H, J = 13.5 Hz) ppm. ^{13}C NMR (major isomer, 75 MHz, CDCl$_3$): δ = 102.8 (CH), 104.0 (CH), 117.2 (CH), 119.5 (C), 121.6 (CH), 122.0 (CH), 125.7 (CH), 126.3 (CH), 129.2 (CH), 129.4 (CH), 130.9 (CH), 131.1 (C), 131.4 (C), 135.5 (C), 137.6 (CH), 140.6 (CH), 142.0 (C), 147.7 (C), 159.7 (C), 166.4 (C), 191.4 (CH), 192.1 (C) ppm. IR (KBr): ν = 1653 (C=O), 1558 (C=C), 1505 (C-O), 1470, 1439, 1330, 1201, 1152 cm^{-1}. HRMS (ESI/ASAP) m/z calculated for C$_{28}$H$_{18}$O$_3$Na [M+Na]$^+$ 425.1154, found 425.1154.

4.16. 5-[2-(4,6-Diphenyl-pyran-2-ylidene)-ethylidene]-cyclopenta[c]thiophene-4,6-dione (14)

The title compound, as a mixture of two (E/Z) isomers with 1:2 ratio (based on integration of ethylenic protons), was obtained following the general procedure and was purified by column chromatography (CH$_2$Cl$_2$/petroleum ether, 2:1). Dark solid (121 mg, 30%). Mp > 260 °C. ^{1}H NMR (major isomer, 300 MHz, CDCl$_3$): δ = 6.94 (d, 1H, J = 0.6 Hz), 6.99 (d, 1H, J = 0.6 Hz), 7.32 (d, 1H, J = 13.5 Hz), 7.50−7.54 (m, 6H), 7.64−7.68 (m, 2H), 7.70−7.73 (m, 2H), 7.90−7.93 (m, 2H), 8.18 (d, 1H, J = 13.5 Hz) ppm. ^{13}C NMR (major isomer, 75 MHz, CDCl$_3$): δ = 103.0 (CH), 104.3 (CH), 117.2 (CH), 125.8 (C), 126.4 (CH), 126.6 (CH), 127.5 (C), 129.3 (CH), 129.4 (CH), 131.0 (CH), 131.5 (CH), 135.3 (C), 139.0 (CH), 146.5 (C), 147.5 (C), 148.4 (C), 160.0 (C), 166.7 (C), 170.0 (C), 184.5 (C), 185.4 (C) ppm. IR (KBr): ν = 1633 (C=O), 1567 (C=C), 1427 (C-O), 1358, 1200, 757 (=C-H), 683 (=C-H) cm^{-1}. HRMS (ESI/ASAP) m/z calculated for C$_{26}$H$_{16}$O$_4$NaS [M+Na]$^+$ 431.0712, found 431.0714.

4.17. 1,3-Dibutyl-5-[2-(4,6-diphenyl-pyran-2-ylidene)-ethylidene]-pyrimidine-2,4,6-trione (15)

The title compound, as a mixture of two (E/Z) isomers with 1:3 ratio (based on integration of ethylenic protons), was obtained following the general procedure and was purified by column chromatography (CH$_2$Cl$_2$/petroleum ether, 2:1). Dark solid (121 mg, 30%). Mp > 260 °C. ^{1}H NMR (major isomer, 300 MHz, CDCl$_3$): δ = 0.88−0.92 (m, 6H), 1.29−1.36 (m, 4H), 1.55−1.59 (m, 4H), 3.84−3.91 (m, 4H), 6.86 (d, 1H, J = 0.6 Hz), 6.97 (d, 1H, J = 0.6 Hz), 7.42−7.50 (m, 7H), 7.55−7.58 (m, 2H), 7.81−7.86 (m, 2H), 8.72 (d, 1H, J = 13.5 Hz) ppm. ^{13}C NMR (major isomer, 75 MHz, CDCl$_3$): δ = 13.8 (CH$_3$), 203 (CH$_2$), 30.4 (CH$_2$), 40.9 (CH$_2$) 41.6 (CH$_2$) 104.3 (CH), 104.5 (C), 104.6 (CH), 117.0 (CH), 125.8 (CH), 126.4 (CH), 129.4 (C), 129.5 (CH), 130.8 (C), 131.2 (CH), 131.7 (CH), 135.1 (C), 147.5 (CH), 149.5 (C), 151.6 (C), 160.5 (C), 163.0 (C), 167.8 (C) ppm. IR (KBr): ν = 2955 (C-H), 1706 (C=O), 1644 (C=C), 1469 (C-O), 1388, 1227, 1197, 758 (=C-H), 683 (=C-H) cm^{-1}. HRMS (ESI/ASAP) m/z calculated for C$_{31}$H$_{32}$N$_2$O$_4$Na [M+Na]$^+$ 519.2254, found 519.2256.

4.18. 4H-Cyclopenta[c]thiophene-4,6(5H)-dione (ThDione, 21)

Thiophene-3,4-dicarboxylic acid anhydride (0.2 g, 1.3 mmol) was dissolved in acetic anhydride (1 mL). Triethylamine (1 mL) and ethylacetoacetate (0.17 mL, 1.31 mmol) were added and the reaction was stirred at 65 °C overnight. The reaction mixture was poured over ice with HCl, the oily product was extracted, dried (Na$_2$SO$_4$), and the solvent was evaporated in vacuo. The resulting carboxylic acid was treated with conc. HCl at reflux for 10 min, cooled to room temperature, and extracted with CH$_2$Cl$_2$ (3 × 50 mL). The combined organic extracts were dried (Na$_2$SO$_4$) and the solvent was evaporated in vacuo. The crude product was suspended in a minimum amount of diethyl ether, stirred at room temperature for 1 h and **21** was filtered off. Yellowish solid (0.14 g, 71%). Mp: 122 °C (dec.). ^{1}H NMR (400 MHz, CDCl$_3$): δ (ppm): 3.54 (s, 2H), 7.99 (s, 2H). ^{13}C NMR (100 MHz, CDCl$_3$): 53.6 (CH$_2$), 125.8 (CH), 148.7 (C), 189.7 (CO). EI-MS (70 eV) m/z (rel. int.): 152 (M$^{+\cdot}$, 100), 110 (75), 96 (50), 82 (50).

Appendix A. Supplementary data

Supplementary data related to this article can be found at http://dx.doi.org/10.1016/j.dyepig.2016.07.008.

References

[1] a) Bureš F. RSC Adv 2014;4:58826−51.
b) Prasad PN, Williams DJ. Introduction to nonlinear optical effects in molecules and polymers. New-York: Wiley-VCH; 1991.
c) Materials for nonlinear optics: chemical perspectives. In: Marder SR, Sohn JE, Stucky GD, editors. ACS symposium series, vol. 455. Washington DC: American Chemical Society; 1991. p. 2.

[2] Kulhánek J, Bureš F, Opršal J, Kuznik W, Mikysek T, Růžička A. Asian J Org Chem 2013;2:422−31.

[3] Jarowski PD, Mo Y. Chem Eur J 2014;20:17214−21.

[4] Moreno-Yruela C, Garín J, Orduna J, Franco S, Quintero E, López Navarrete JT, et al. J Org Chem 2015;80:12115−28.

[5] a) Marder SR, Cheng LT, Tiemann BG, Friedli AC, Blanchard-Desce M, Perry JW, et al. Science 1994;263:511−4.
b) Marder SR, Berantan DN, Chen LT. Science 1991;252:13−106.

[6] a) Achelle S, Kahlal S, Saillard J-Y, Cabon N, Caro B, Robin-le Guen F. Tetrahedron 2014;70:2804−15.
b) Ba F, Cabon N, le Poul P, Kahlal S, Saillard J-Y, le Poul N, et al. New J Chem 2013;37:2066−81.
c) Ba F, Cabon N, Robin-le Guen F, le Poul P, le Poul N, le Mest Y, et al. Organometallics 2008;27:6396−9.

[7] See for example. a) Marco AB, Martínez de Baroja N, Franco S, Garín J, Orduna J, Villacampa B, et al. Chem. Asian J 2015;10:188−97.
b) Marco AB, Mayorga Burrezo P, Mosteo L, Franco S, Garín J, Orduna J, et al. Rsc Adv 2015;5:231−42.
c) Gauthier S, Voogdin N, Achelle S, Barsella A, Caro B, Robin-le Guen F. Tetrahedron 2013;69:8392−9.
d) Achelle S, Malval J-P, Aloïse S, Barsella A, Spangenberg A, Mager L, et al. ChemPhysChem 2013;14:2725−36.
e) Poronik YM, Hugues V, Blanchard-Desce M, Gryko DT. Chem.-Eur J 2012;18:9258−66.
f) Andreu R, Galan E, Orduna J, Villacampa B, Alicante R, López Navarrete JT, et al. Chem.-Eur J 2011;17:826−38.
g) Andreu R, Galan E, Garín J, Herrero V, Lacarra E, Orduna J, et al. J Org Chem 2010;75:1684−92.
h) Andreu R, Carrasquer L, Franco S, Garín J, Orduna J, Martínez de Baroja N, et al. J Org Chem 2009;74:6647−57.

[8] See for example. a) Gauthier S, Caro B, Robin-le Guen F, Bhuvanesh N, Gladysz JA, Wojcik L, et al. Dalton Trans 2014;43:11233−42.
b) Pérez Tejada R, Pellejà L, Palomares E, Franco S, Orduna J, Garín J, et al. Org Electron 2014;15:3237−50.
c) Franco S, Garín J, Martínez de Baroja N, Pérez-Tejada R, Orduna J, Yu Y, et al. Org Lett 2012;14:752−5.
d) Bolag A, Nishida J, Hara K, Yamashita Y. Org Electron 2012;13:425−31.

[9] a) Hales JM, Matichak J, Barlow S, Chira S, Yesudas K, Brédas J-L, et al. Science 2010;327:1485−8.
b) Faux N, Robin-le Guen F, le Poul P, Caro B, Nakatani K, Ishow E, et al. Eur J Inorg Chem 2006;3489−97.
c) Faux N, Caro B, Robin-le Guen F, le Poul P, Nakatani K, Ishow E. J Organomet Chem 2005;690:4982−8.

[10] See for example. a) Gupta VK, Singh RA. RSC Adv 2015;5:38591−600.
b) Kim YJ, Lee GB, Jeon CW, Kim YH, Chung DS, Park CE. RSC Adv 2015;5:3435−42.
c) Yalçın E, Achelle S, Bayrak Y, Seferoğlu N, Barsella A, Seferoğlu Z. Tetrahedron Lett 2015;56:2586−9.
d) Morales AR, Frazer A, Woodward AW, Ahn-White HY, Fonari A, Tongwa P, et al. J Org Chem 2013;78:1014−25.

[11] a) Solanke P, Bureš F, Pytela O, Klikar M, Mikysek T, Mager L, et al. Eur J Org Chem 2015:5339−49.
b) Zitzler-Kunkel A, Lenze MR, Schnier T, Meerholz K, Wurthner F. Adv Funct Mater 2014;24:4645−53.
c) Bordone F, Carella A, Ricciotti L, Tuzi A, Roviello A, Barsella A. Dyes Pigm 2011;88:290−5.
d) Andreu R, Aramburo J, Cerdan MA, Garín J, Orduna J, Villacampa B. Tetrahedron Lett 2006;47:661−4.

[12] See for example. a) Kulinich AV, Mikitenko EK, Ishchenko AA. *Phys Chem Chem Phys* 2016;18:3444−53.
b) Klikar M, Bureš F, Pytela O, Miysek T, Padělková Z, Barsella A, et al. New J Chem 2013;37:4230−40.
c) Tehfe M-A, Dumur F, Graff B, Morley-Savary F, Gigmes D, Fouassier J-P, et al. Polym Chem 2013;4:3866−75.
d) Castro MCR, Belsley M, Fonseca AMC, Raposo MMM. Tetrahedron 2012;68.8147−4153.
e) Moran AM, Delbecque C, Kelley AM. J Phys Chem A 2001;105:10208−19.

[13] a) Sekar N, Umape PG, Patil SR. J Fluoresc 2015;25:1787−800.
b) Kovalski K, Szczupak L, Skiba J, Abdel-Rahman OS, Winter RF, Czerwieniec R, et al. Organometallics 2014;33:4697−705.

[14] a) Raimundo J-M, Blanchard P, Frère P, Mercier N, Ledoux-Rak I, Hierleb R, et al. Tetrahedron Lett 2001;42:1507−10.
b) Raimundo J-M, Blanchard P, Ledoux-Rak I, Hierle R, Michaux L, Roncali J. Chem Commun 2000:1597−8.
c) Alain V, Blanchard-Desce M, Chen C, Marder S, Fort A, Barzoukas M. Synth Met 1996;81:133−6.

[15] Solanke P, Bureš F, Pytela O, Kulhanek J, Padelkova Z. Synthesis 2013;45:3044−51.

[16] a) Wadsworth DH, Detty MR, Murray BJ, Weidner CH, Haley NF. J Org Chem 1984;49:2676−81.
b) Reynolds GA, Van Allan JA. J Org Chem 1969;34:2736−41.

[17] Nielsen CB, Bjørnholm T. Org Lett 2004;6:3381−4.

[18] Cheng LT, Tam W, Stevenson SH, Meredith GR, Rikken G, Marder SR. J Phys Chem 1991;95:10631−43.

[19] a) Jen AKY, Cain Y, Redworth PV, Marder SR. Adv Mater 1997;9:132−5.
b) Marguerettaz X, O'neill R, Fitzmaurice D. J Am Chem Soc 1994;116:2629−30.

[20] Gaussian 09, Revision D.01, M. J. Frisch, G. W. Trucks, H. B. Schlegel, G. E. Scuseria, M. A. Robb, J. R. Cheeseman, et al, Gaussian, Inc, Wallingford CT, 2013.

[21] ArgusLab 4.0, Mark A. Thompson, Planaria Software LLC, Seattle, WA. http://www.arguslab.com.